

for X-Ray Crystallography<sup>33</sup> for the other atoms and those for W and P were corrected for anomalous dispersion. The details of data collection are included in Table III.

The position of the W was derived from the Patterson map, and the Fourier map phased on W revealed the remainder of the complex. All H atoms were introduced into the model with fixed coordinates at idealized positions and isotropic  $U = 0.076 \text{ \AA}^2$ . Least-squares refinement of the non-hydrogen atoms with anisotropic  $U_{ij}$ 's, minimizing  $\sum w[F_o^2 - (F_c/k)^2]^2$ ,<sup>34</sup> using all the data (5728 reflections) led to  $S$  (goodness of fit) = 1.27 and  $R_F = 0.043$ ; final shift/errors < 0.01. The maximum deviations found in the  $\Delta\rho$  map are close to  $W$  and are about  $1.2 \text{ e \AA}^{-3}$ . All calculations were carried out on a VAX 11/780 computer using the CRYRM system of programs.

### Equilibrium Studies

Initial concentrations of **2** were based on the integrated peak areas with respect to added alcohol at time  $t = 0$ . Subsequent

(33) "International Tables for X-ray Crystallography"; Kynoch Press: Birmingham, England, 1974; Vol. IV.

(34) The weights,  $w = [s + r^2b + (0.02s)^2]^{-1}(Lp/k^2)^2$ ,  $s$  = scan counts,  $r$  = scan-to-background time ratio,  $b$  = total background counts,  $k$  = scale factor of  $F$ ;  $R_F = \sum |F_o - |F_c|| / \sum |F_o|$  (sums of reflections with  $I > 0$ );  $+ R'_F = R_F$  (sums of reflections with  $I > 3\sigma(I)$ );  $S = [\sum w(F_o^2 - (F_c/k)^2)^2 / (n - v)]^{1/2}$ ,  $n$  = number of reflections,  $v$  = number of parameters.

concentrations of **2** and **5** were established by the percentage of the integrated signal intensities of the relevant Cp proton signals in relation to that of the total Cp integration. Temperatures were determined by measurement of  $\Delta\nu(\text{MeOH})$  with use of equation

$$T(\text{K}) = 406.0 - 0.551|\Delta\nu| - 63.4(\Delta\nu/100)^2$$

$\Delta\nu$  is the difference in Hz between the chemical shifts of the OH and  $\text{CH}_3$  signals. The above equation is for 60-MHz values; 90-MHz values must be corrected accordingly.<sup>35</sup>

**Acknowledgment** is made to the Southern California Regional High Field NMR Facility supported by the NSF and to the Department of Energy (Contract No. DE-AM03-76SF00767) for support of this research. We thank J. D. Meinhart for 500-MHz  $^1\text{H}$  NMR and difference NOE spectra.

**Supplementary Material Available:** Tables of H-atom coordinates (Table VIII), Gaussian amplitudes (Table IX), and a listing of structure factor amplitudes (Table X) (32 pages). Ordering information is given on any current masthead page.

(35) Gordon, A. J.; Ford, R. A. "The Chemist's Companion"; Wiley: New York, 1972.

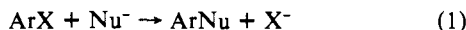
## Electron-Transfer-Induced Reactions. A Novel Approach Based on Electrochemical Redox Catalysis. Application to Aromatic Nucleophilic Substitutions

Christian Amatore,<sup>1a</sup> Mehmet A. Oturan,<sup>1b</sup> Jean Pinson,<sup>1a</sup> Jean-Michel Savéant,<sup>\*1a</sup> and André Thiébaud<sup>1b</sup>

Contribution from the Laboratoire d'Electrochimie de l'Université Paris 7, 75 251 Paris Cedex 05, France, and the Laboratoire de Chimie Analytique des Milieux Réactionnels Liquides, ESPCI, 75 231 Paris Cedex 05, France. Received November 28, 1983

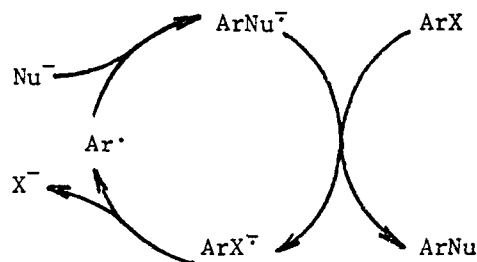
**Abstract:** A novel approach based on redox catalysis for electrochemical induction of aromatic nucleophilic substitution is presented. The advantages of this method over the conventional ones are discussed in terms of kinetic and preparative scopes. The capabilities of the method for determining the kinetics of fast nucleophilic attack on an aromatic radical in the context of aromatic nucleophilic substitution is illustrated with the example of the reaction of 2-chlorobenzonitrile with benzenethiolate.

Current interest in aromatic nucleophilic substitutions stems from their important synthetic capabilities.<sup>2</sup> Unfortunately the direct reaction



although thermodynamically possible is often so slow as to be practically impossible. Activation of the reaction via photochemistry or by chemical or electrochemical reduction leads to a considerable increase<sup>2</sup> of the global rate of reaction 1. It is therefore of utmost importance to understand the mechanism of these activation processes. In this connection it has been shown in the past few years<sup>3</sup> that a complete description of the mechanism was attainable by the use of readily available transient electro-

Scheme I



chemical techniques. Owing to the recent development of electron-transfer-catalyzed reactions,<sup>4</sup> the relevance of these studies to other processes in organic chemistry as well as in coordination and organometallic chemistry is obvious.

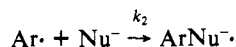
(1) (a) Laboratoire d'Electrochimie de l'Université Paris 7. (b) Laboratoire de Chimie Analytique des Milieux Réactionnels Liquides de l'ESPCI.

(2) (a) Rossi, R. A.; De Rossi, R. H. "Aromatic Substitution by the SRN1 Mechanism"; American Chemical Society: Washington, 1983; ACS Monographs. (b) Wolfe, J. F.; Carver, D. R., *Org. Prep. Proced. Int.* **1978**, *10*, 225. (c) Bunnett, J. F. *Acc. Chem. Res.* **1978**, *11*, 413. (d) Savéant, J. M. *Acc. Chem. Res.* **1980**, *13*, 323. (e) Boujlel, K.; Simonet, J.; Roussi, G.; Beugelmans, R. *Tetrahedron. Lett.* **1982**, *23*, 173.

(3) (a) Pinson, J.; Savéant, J. M. *J. Chem. Soc., Chem. Commun.* **1974**, 933. (b) Pinson, J.; Savéant, J. M. *J. Am. Chem. Soc.* **1978**, *100*, 1506. (c) Amatore, C.; Savéant, J. M.; Thiébaud, A. *J. Electroanal. Chem.* **1979**, *103*, 303. (d) Amatore, C.; Chaussard, J.; Pinson, J.; Savéant, J. M.; Thiébaud, A. *J. Am. Chem. Soc.* **1979**, *101*, 6012. (e) Amatore, C.; Pinson, J.; Savéant, J. M.; Thiébaud, A. *J. Electroanal. Chem.* **1980**, *107*, 59; **1980**, *107*, 75; **1981**, *123*, 231. (f) Amatore, C.; Pinson, J.; Savéant, J. M.; Thiébaud, A. *J. Am. Chem. Soc.*, **1981**, *103*, 6930; **1982**, *104*, 817. (g) Reference 2d.

(4) Reference 2d and the following: (a) Hersberger, J. W.; Klinger, R. J.; Kochi, J. K. *J. Am. Chem. Soc.* **1983**, *105*, 61. (b) Hersberger, J. W.; Amatore, C.; Kochi, J. K. *J. Organomet. Chem.* **1983**, *250*, 345. (c) Kochi, J. K. "Organometallic Mechanisms and Catalysis"; Academic Press: New York, 1978. (d) Chanon, M.; Tobe, M. L. *Angew. Chem., Int. Ed. Engl.* **1982**, *21*, 1. (e) Ebersson, L. *Adv. Phys. Org. Chem.* **1982**, *18*, 79. (f) Alder, R. W. *J. Chem. Soc., Chem. Commun.* **1980**, 1184. (g) Amatore, C.; Badoz-Lambling, J.; Bonnel-Huyghes, C.; Pinson, J.; Savéant, J. M.; Thiébaud, A. *J. Am. Chem. Soc.* **1982**, *104*, 1979. (h) Lexa, D.; Savéant, J. M. *J. Am. Chem. Soc.* **1982**, *104*, 3503. (i) Julliard, M.; Chanon, M. *Chem. Rev.* **1983**, *83*, 425.

Let us recall briefly the essential features of the direct electrochemical activation of  $S_{RN}1$  reactions. Reduction of the haloaromatic by an electrode leads to its anion radical which starts the catalytic cycle in Scheme I, which should normally propagate to convert all the haloaromatic into its substitution product  $ArNu$  according to the balance eq 1. However, the efficiency of the whole process mainly depends on the nature and rates of the termination steps.<sup>5</sup> Among the most important<sup>6</sup> termination reactions are the reduction of  $Ar\cdot$  by the electrode or  $ArX\cdot$  or  $ArNu\cdot$  leading to the corresponding aromatic after protonation of  $Ar\cdot$ . One of the main results of interest here is that the yield in  $ArNu$  depends on the magnitude of the rate constant,  $k_1$ , of the cleavage of the anion radical  $ArX\cdot$ . This can be rationalized as follows.<sup>7</sup> When  $k_1$  is large enough,  $Ar\cdot$  is produced close to the electrode which mainly reduces it; thus the larger  $k_1$  the lower the yield in  $ArNu$ .<sup>8</sup> When  $k_1$  is smaller,  $Ar\cdot$  is formed in the solution and is mainly reduced by  $ArX\cdot$ ; thus the larger  $k_1$  the lower the concentration of  $ArX\cdot$ , and thus the higher the yield in  $ArNu$ .<sup>9</sup> This is a built-in problem of the usual electrochemical approach as soon as one is concerned with the preparative aspect of the reaction. However, for kinetic purposes these situations may lead to an easy characterization of the overall kinetics as well as the determination of either  $k_1/k_2$  ( $k_1$  large) or  $k_2k_1^{1/2}$  ( $k_1$  smaller) where  $k_2$  is the rate constant of the nucleophilic attack in the  $\sigma$ -aromatic radical  $Ar\cdot$ .<sup>3</sup>



This, however, can lead to the value of  $k_2$  only when  $k_1$  can be determined independently. Owing to difficulties in measuring  $k_1$  for a number of poorly activated haloaromatics,<sup>10</sup> this appears as a limitation of the direct electrochemical method as soon as one looks for  $k_2$  evaluation.

This limitation can, however, be easily overcome via a new approach based on redox catalysis<sup>11</sup> of the electrochemical activation. This approach was suggested by one of us in a review paper summarizing the past work of our group on the electrochemical inducement of aromatic nucleophilic substitution.<sup>2d</sup> See also the description of an earlier application of redox catalysis in the particular case where the catalyst couple is  $ArNu/ArNu\cdot$ , i.e., derives from the substitution product itself.<sup>3f,12</sup> During the submission of the present paper, we received communication of a paper submitted to the same journal which describes the successful preparation of diphenyl thioether from bromobenzene and benzenethiolate using benzonitrile as the redox catalyst.<sup>13</sup> The

(5) See, e.g., ref 3f.

(6) (a) In a good H atom donor medium, an additional termination step involves and H atom transfer to  $Ar\cdot$  from the solvent/supporting electrolyte system. See, e.g., ref 2d, 3f, and the following: M'Halla, F.; Pinson, J.; Savéant, J. M. *J. Am. Chem. Soc.* **1980**, *102*, 4120. (b) Another possible termination step can be related to the reversibility of the nucleophilic attack or parallel chemical evolution of  $ArNu\cdot$ ; see, e.g.; Rossi, R. A.; Palacios, S. M. *J. Org. Chem.* **1981**, *46*, 5300; ref 2a.

(7) In electrochemistry, the  $k_1$  effect on the  $ArNu$  yield arises mainly from the heterogeneous nature of the solution near the electrode. However, such dependence on  $k_1$  can also be found for purely homogeneous processes (see, e.g., ref 3f).

(8) The yield in  $ArNu$  depends then only on  $k_2[ArNu\cdot]/k_1$ , and the situation is described as "heterogeneous" to emphasize that the main termination step is the reduction of  $Ar\cdot$  by the electrode.

(9) (a) The situation is termed to be "homogeneous". The yield in  $ArNu$  then depends only on the magnitude of  $k_2[ArNu\cdot]/k_1$ , where (b)  $k_2$  is the diffusion limit rate constant and  $\theta$  is the characteristic time of the method ( $\theta = RT/Fv$  in cyclic voltammetry,  $v =$  scan rate;  $\theta = \delta^2/D$  in preparative scale electrolysis,  $\delta =$  diffusion layer thickness,  $D =$  average diffusion coefficient).

(10) Transient electrochemical methods allow an easy determination of  $k_1$  up to  $10^6$  s<sup>-1</sup>. However, most of the haloaromatic substrates of interest correspond to  $k_1$  far above this limit. Redox catalysis<sup>11</sup> may extend this limit when special requirements are met.

(11) (a) Andrieux, C. P.; Blocman, C.; Dumas-bouchiat, J. M.; Savéant, J. M. *J. Am. Chem. Soc.* **1979**, *101*, 3431. (b) Andrieux, C. P.; Blocman, C.; Dumas-Bouchiat, J. M.; M'Halla, F.; Savéant, J. M. *J. Am. Chem. Soc.* **1980**, *102*, 3806.

(12) Amatore, C.; Pinson, J.; Savéant, J. M.; Thiébaud, A. *J. Electroanal. Chem.* **1980**, *107*, 59.

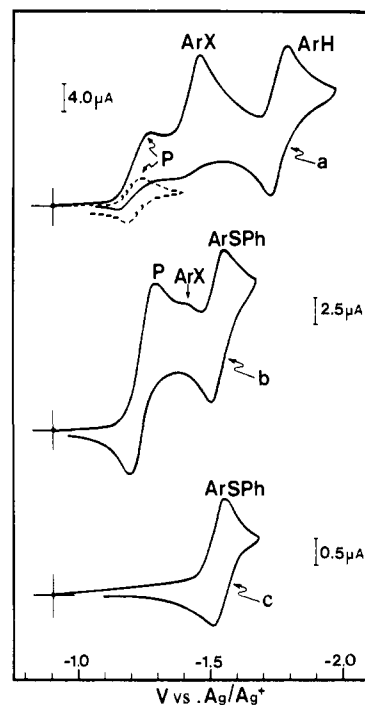


Figure 1. Cyclic voltammetry of (a) 4-cyanopyridine ( $2.2 \times 10^{-3}$  M) in the absence (dashed line) or in the presence of  $8.9 \times 10^{-3}$  M 2-chlorobenzonitrile (full line), (b) 4-cyanopyridine ( $6.6 \times 10^{-3}$  M) in the presence of  $8.9 \times 10^{-3}$  M 2-chlorobenzonitrile and  $3.5 \times 10^{-2}$  M  $PhS^-$ , and (c) 2-chlorobenzonitrile ( $1.4 \times 10^{-3}$  M) in the presence of 1.0 M  $PhS^-$ . Gold electrode; liquid  $NH_3$  at  $-40^\circ C$  with 0.1 M  $KBr$ ,  $v = 0.2$  V s<sup>-1</sup>.

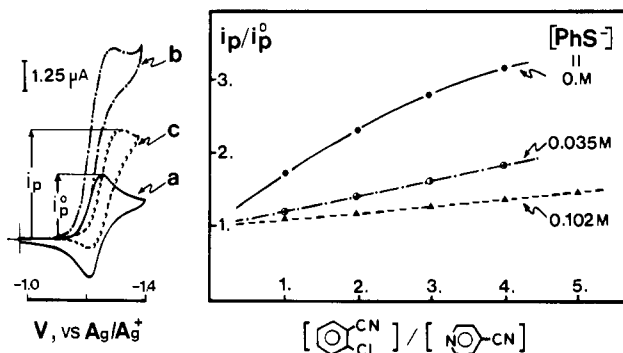


Figure 2. Variations of the current peak intensity of the 4-cyanopyridine ( $2.3 \times 10^{-3}$  M) wave in the presence of various amounts of 2-chlorobenzonitrile and benzenethiolate ion, in liquid ammonia, at  $-40^\circ C$ , at a mercury electrode ( $v = 0.11$  V s<sup>-1</sup>). (a-c) Cyclic voltammograms of 4-cyanopyridine in the same conditions: (a) alone; (b) with  $6.7 \times 10^{-3}$  M 2-chlorobenzonitrile added; (c) same as part b with 0.035 M  $PhS^-$  added.

aim of the work described hereafter was to evaluate the redox catalytic approach for kinetic purposes in comparison with the direct electrochemical method and to discuss the advantages and limitation of the redox catalytic approach for preparative scopes.

## Results

Let us first present the principle of the method for the determination of rapid second-order rate constant, with the example of the substitution of 2-chlorobenzonitrile by benzenethiolate in liquid ammonia, the redox catalyst being 4-cyanopyridine. Figure 1a presents the voltammogram of the catalyst (P) alone (dashed curve) or in the presence of 2-chlorobenzonitrile ( $ArX$ ). It is seen that the presence of the haloaromatic results in a dramatic enhancement of the cathodic peak of the catalyst wave together with a loss of the reversibility, i.e., disappearance of the anodic peak.

(13) Swartz, J. E.; Stenzel, T. T. *J. Am. Chem. Soc.* **1984**, *106*, 2520.

This trend is typical of redox catalysis and corresponds to the overall reduction of the ArX into ArH at the level of the catalyst wave.<sup>11</sup> Figure 1b shows that this effect almost cancels when PhS<sup>-</sup> is added to the medium as evidenced by the reappearance of the anodic peak of the P wave; on the other hand, it is seen that the ArH wave is no longer observed and a new wave develops corresponding to the substitution product, ArSPh, as evidenced by comparison with Figure 1c, and with the voltammogram of an authentic sample. At a first glance everything happens as if the addition of PhS<sup>-</sup> was destroying the redox catalysis phenomenon, restoring the original CV trace for the catalyst. However, the phenomena is clearly more complex as shown by the appearance of the ArSPh wave.

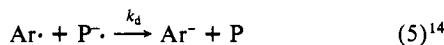
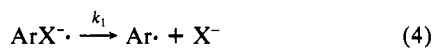
Figure 2 illustrates in a more systematic way the dependence of the phenomenon on either the ArX or the PhS<sup>-</sup> concentrations. This is represented under the form of the variations of  $i_p/i_p^0$  as a function of these two factors ( $i_p$  and  $i_p^0$  are the current peak heights of the 4-cyanopyridine (P) cathodic wave, in the presence or in the absence of PhS<sup>-</sup>, respectively, for the same experimental conditions, i.e., same scan rate, same ArX and P concentration, at the same electrode). This shows that the effects observed in Figure 1b increase when more and more PhS<sup>-</sup> is introduced into the medium.

### Discussion

**Redox Catalysis in the Absence of PhS<sup>-</sup>.** Since redox catalysis is now a well-documented phenomenon<sup>11</sup> we will just recall its basic principles. In the absence of any haloaromatic, the 4-cyanopyridine (P) gives rise to a perfectly reversible CV wave (Figure 1a) corresponding to the one-electron transfer:

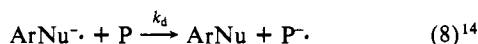
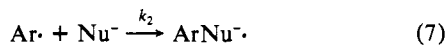


When the 2-chlorobenzonitrile (ArX) is added to the solution, the anion radical P<sup>-</sup> homogeneously reduces it according to the sequence



Note that the formally endergonic electron transfer (eq 3) is continuously displaced by the irreversible cleavage of the frangible anion radical ArX<sup>-</sup> (eq 4). This latter reaction gives the  $\sigma$ -aromatic radical Ar<sup>•</sup> which is in turn reduced by P<sup>-</sup> leading thus to an overall 2-electron process per molecule of ArX initially reduced. Thus the current peak of the 4-cyanopyridine increases, and since P<sup>-</sup> is consumed the reversibility of the P wave disappears.

**Redox Catalysis in the Presence of PhS<sup>-</sup>.** The strong affinity of PhS<sup>-</sup> for Ar<sup>•</sup> is evidenced by the disappearance of the ArX and ArH CV peaks on the voltammogram b in Figure 1. This corresponds<sup>2d,3</sup> to the electrocatalysis of eq 1, according to the sequence of Scheme I. Thus when PhS<sup>-</sup> is added to the system containing 2-chlorobenzonitrile and 4-cyanopyridine a similar phenomenon develops according to



together with the initial steps 2–4.

When reaction 7 totally overcomes reaction 5 the whole sequence is clearly catalytic, the initial 4-cyanopyridine anion radical, P<sup>-</sup>, consumed in step 3, being brought back by reaction 8. Thus no redox catalytic effect is observed for the CV wave of 4-cyanopyridine, i.e.,  $i_p/i_p^0$  tends back toward one and the anodic peak featuring the P<sup>-</sup> reoxidation shows up again. The overall process thus appears as if the system was behaving according to the single eq 2, except that now the ArNu wave is observed at

**Table I.<sup>a</sup>** Rate Constants for the Nucleophilic Attack of PhS<sup>-</sup> on the 2-Benzonitrile Radical, As Determined by Redox Catalysis with 4-Cyanopyridine as Redox Catalyst

	[2-chlorobenzonitrile]/ [4-cyanopyridine]				
	1.0	2.0	3.0	4.0	5.0
[4-cyanopyridine] = 2.32 × 10 <sup>-3</sup> M, [PhS <sup>-</sup> ] = 0.102 M					
log $k_2^b$					
$v = 0.11$ V s <sup>-1</sup>		9.72	9.68	9.67	9.68
$v = 0.20$ V s <sup>-1</sup>		9.94	9.95	9.78	9.90
$v = 0.29$ V s <sup>-1</sup>			10.30	10.15	10.11
[4-cyanopyridine] = 4.03 × 10 <sup>-3</sup> M, [PhS <sup>-</sup> ] = 0.102 M					
log $k_2^b$					
$v = 0.11$ V s <sup>-1</sup>					9.68
$v = 0.20$ V s <sup>-1</sup>					9.97
$v = 0.29$ V s <sup>-1</sup>					10.0
[4-cyanopyridine] = 6.10 × 10 <sup>-3</sup> M, [PhS <sup>-</sup> ] = 0.102 M					
log $k_2^b$					
$v = 0.11$ V s <sup>-1</sup>					10.45
[4-cyanopyridine] = 2.18 × 10 <sup>-3</sup> M, [PhS <sup>-</sup> ] = 3.56 × 10 <sup>-2</sup> M					
log $k_2^b$					
$v = 0.11$ V s <sup>-1</sup>	9.81	9.70	9.62		
$v = 0.20$ V s <sup>-1</sup>	9.74	9.83	9.75		
$v = 0.29$ V s <sup>-1</sup>	9.67	9.85	9.84		
[4-cyanopyridine] = 6.59 × 10 <sup>-3</sup> M, [PhS <sup>-</sup> ] = 3.56 × 10 <sup>-2</sup> M					
log $k_2^b$					
$v = 0.11$ V s <sup>-1</sup>	9.67				
$v = 0.20$ V s <sup>-1</sup>	9.65				
$v = 0.29$ V s <sup>-1</sup>	9.67				

<sup>a</sup> In liquid ammonia at -40 °C, 0.1 M KBr, at a mercury electrode.  
<sup>b</sup> For  $k_d = 3 \times 10^{10}$  M<sup>-1</sup> s<sup>-1</sup>.

more cathodic potentials showing that the whole sequence eq 2–4, 7, 8 has taken place.

In an intermediate situation reaction 5 competes with reaction 7 for Ar<sup>•</sup> consumption. Thus the 4-cyanopyridine wave still possesses a marked redox catalysis character, although diminished as compared to the case in the absence of PhS<sup>-</sup>. This decrease is related directly to the value of the effective rates of eq 5 and 7 for Ar<sup>•</sup> consumption, i.e., to the parameter:  $(k_2[Nu^-])/(k_d[P]_0)$ . On the basis of this formulation, the advantage of the method for kinetic purposes over the direct electrochemical method clearly appears, since it allows direct access to the ratio  $k_2/k_d$  where  $k_d$  is the diffusion-limit second-order rate constant ( $k_d \approx 3 \times 10^{10}$  M<sup>-1</sup> s<sup>-1</sup> in liquid NH<sub>3</sub> at -40 °C<sup>3</sup>).

Treatment of the data in the absence of PhS<sup>-</sup> shows that the redox catalytic phenomenon is controlled<sup>11</sup> by the rate of the forward electron transfer  $k_0 = 9.5 \times 10^2$  M<sup>-1</sup> s<sup>-1</sup>. With this value measured independently, the variation of  $i_p/i_p^0$  (see, e.g., Figure 2) with the scan rate,  $v$ , and the 4-cyanopyridine, 2-chlorobenzonitrile, and benzenethiolate concentrations affords the value of  $k_2 = (6.1 \pm 0.7) \times 10^9$  M<sup>-1</sup> s<sup>-1</sup> for the rate of PhS<sup>-</sup> attack on the 2-benzonitrile radical. Table I shows the consistency of the results obtained for these different conditions although a slight systematic increase of  $k_2$  is observed with the scan rate at the highest PhS<sup>-</sup> concentration. Since this trend is not observed for PhS<sup>-</sup> = 3.56 × 10<sup>-2</sup> M and no consistent deviation is observed with either the 4-cyanopyridine or the 2-chlorobenzonitrile concentrations, we consider that this effect is due to experimental uncertainty owing to the fact that  $i_p/i_p^0$  values are close to one at the highest PhS<sup>-</sup> concentration<sup>15</sup> (see, e.g., Figure 2).

(14) Owing to the large exergonicity of this electron transfer, its rate constant is considered as being close to the diffusion limit rate constant.

(15) (a) Table I includes all the data obtained on this system. However, for the largest scan rates and PhS<sup>-</sup> concentration and the smallest 4-cyanopyridine concentrations, the accuracy on  $(i_p/i_p^0)$  measurements introduces high errors on  $k_2$  since this ratio tends toward unity in these conditions (see Figure 2). One referee suggested that this systematic deviation for  $k_2$  was due to the possible evolution of the radical anion of the substitution product. However, this hypothesis is clearly ruled out in this case since the CV of the substitution product is perfectly reversible in the CV time scale considered here (see, e.g., Figure 1c).

The above example illustrates the power of this approach for kinetic purposes. Let us now discuss the potentialities of this method for preparative scopes. As summarized above, in poor H atom donor solvents the main deactivation steps for the chain reaction in Scheme I are the various possible pathways for Ar-reduction.<sup>6</sup> For the approach based on redox catalysis, the yield in ArNu thus depends on the parameter  $k_2[\text{Nu}^-]/(k_d[\text{P}]_0)$  whereas it depends<sup>2</sup> on  $k_2[\text{Nu}^-]/k_1$  (when<sup>16,9b</sup>  $k_1 \gg (k_d[\text{ArX}]_0)^{2/3}\theta^{-1/3}$ ) or on  $k_2[\text{Nu}^-]k_1^{1/2}\theta^{1/2}/(k_d[\text{ArX}]_0)$  (for the converse situation) in the context of the direct electrochemical approach. It is thus seen that the approach via redox catalysis will be preferable when either  $k_1 \gg k_d[\text{P}]_0$  (for large  $k_1$ ) or  $k_1\theta \ll ([\text{ArX}]_0/[\text{P}]_0)^2$  (for smaller  $k_1$ ). Obviously the latter condition is not truly realistic since the redox catalysis phenomenon needs  $k_1\theta \gg 1$  to be effective.<sup>17</sup> Thus we can conclude that the approach based on redox catalysis will be advantageous when compared to the direct method as soon as  $k_1 \gg k_d[\text{P}]_0$ , i.e., for the cases involving very frangible anion radicals, such as  $\text{PhX}^-$ , X = Cl, Br, I.<sup>2,13</sup> When the converse situation is obtained the direct approach is preferable for preparative scopes.

(16) Amatore, C.; Savéant, J. M. *J. Electroanal. Chem.* 1977, 85, 27.

(17) This condition corresponds to a fast irreversible cleavage of  $\text{ArX}^-$  in the time scale considered. This requirement is needed to allow a continuous displacement of the reversible electron transfer in eq 3. See ref 11.

However, as exemplified by the example of 2-chlorobenzonitrile with  $\text{PhS}^-$  presented in this paper, the approach based on redox catalysis may be extremely worthwhile as a kinetic tool for determination of rates of nucleophilic attack close to the diffusion limit. Application of this method to the comparative investigation of the reactivity in an extended series of Ar-/nucleophile systems is currently in progress.

#### Experimental Section

The experimental setup, electrochemical cell, and procedures for purifying the solvent were the same as previously described.<sup>3d</sup> The working electrode for the CV in Figure 1 was a gold disk of diameter 1 mm, polished on alumina before use. The data in Figure 2 and in Table I were obtained at a hanging mercury drop for a lesser contribution of the background current and capacitive current on the  $i_p$  and  $i_p^0$  measurements. The reference electrode was an Ag/Ag<sup>+</sup> 0.01 M electrode in liquid ammonia. The supporting electrolyte was KBr, 0.1 M.

The starting materials were from commercial origin. 2-Chlorobenzonitrile was sublimed prior to use.

2-Cyanodiphenyl sulfide was prepared by refluxing for 15 h 0.01 mol of 2-chlorobenzonitrile and 0.01 mol of sodium benzenethiolate in DMF. After filtration of NaCl and evaporation of the solvent, the white product was purified by recrystallization in dilute methanol, mp 58 °C. Anal.: mass spectrum ( $m/e$ ) 213 (5), 212 (18), 211 (100), 210 (43), 185 (8), 184 (34), 183 (5), 109 (13), 108 (10), 92 (11), 77 (34).

Registry No. 2-Chlorobenzonitrile, 873-32-5; benzenethiolate, 13133-62-5; 4-cyanopyridine, 100-48-1.

## Molecular Environment Effects in Redox Chemistry. Reversible Multielectron Oxidation of Amide-Linked, Basket-Handle Metalloporphyrins

Doris Lexa,<sup>1a</sup> Philippe Maillard,<sup>1a,c</sup> Michel Momenteau,<sup>1b</sup> and Jean-Michel Savéant<sup>1a\*</sup>

Contribution from the Laboratoire d'Electrochimie de L'Université Paris 7, 75251 Paris Cedex 05, France, and the Institut Curie, Section Biologie, Unité Inserm 219, Centre Universitaire, bat.122, 91405 Orsay, France. Received January 6, 1984

**Abstract:** Electrochemical oxidation of Cu, Zn, and Mg amide-linked, basket-handle porphyrins involves the simultaneous reversible uptake of two electrons leading directly to the dication as opposed to what happens with the parent tetraphenylporphyrin (TPP) complexes where two one-electron steps separated by several hundreds of millivolts are observed. Comparison with tetra-*o*-methoxy- and tetra-*o*-nitro-substituted TPP and with ether-linked, basket-handle porphyrin complexes shows that this is a manifestation of the presence of amide groups in the chains. Amide-linked, basket-handle Cu and Mg dimers bound by two NHCONH groups undergo a simultaneous four-electron reversible uptake leading directly to the dimeric tetracation. Possible reasons for this new and spectacular effect of the amide groups located in the immediate vicinity of the porphyrin ring are discussed.

It has been shown previously<sup>2</sup> that the presence of ether-linked or amide-linked, basket-handle chains exerts a pronounced influence on the redox and coordination chemistry of iron porphyrins. Of particular interest is the behavior exhibited by the amide-linked compounds owing to their approximate resemblance with metalloproteins. It was observed that the negatively charged complexes formed upon successive reduction of the starting Fe<sup>III</sup> porphyrins are destabilized by the presence of the ether-linked chains as a result of steric hindrance to solvation. The same effect also exists with the amide-linked, basket-handle complexes but is overcompensated by dipolar interactions with the NHCO groups

acting as acceptors. An overall stabilization of the negatively charged species ensues resulting in opposite shifts of standard potentials and complexation constants as compared to what happens with the ether-linked derivatives.

In the present preliminary report, we describe an even more spectacular effect of amide-linked, basket-handle structures on the redox chemistry of metalloporphyrins. It concerns the formation upon electrochemical oxidation of the cation radicals and the dications of Cu, Zn, and Mg porphyrins.

With the standard tetraphenylporphyrin (TPP) complexes, two well-separated, one-electron reversible electron-transfer steps<sup>3</sup> are

(1) (a) Université Paris 7. (b) Institut Curie, Orsay. (c) Presently at the Institut Curie.

(2) Lexa, D.; Momenteau, M.; Rentien, P.; Rytz, G.; Savéant, J. M.; Xu, F. *J. Am. Chem. Soc.*, in press.

(3) (a) Stanienda, A.; Biebl, G. *Z. Phys. Chem. (Weisbaden)* 1967, 52, 254. (b) Wolberg, A.; Manassen, J. *J. Am. Chem. Soc.* 1970, 92, 2982. (c) Carineri, N.; Harriman, A. *Inorg. Chim. Acta* 1982, 62, 103. (d) Kadish, K. M.; Shine, L. R. *Inorg. Chem.* 1982, 21, 3623.